TWO-TEMPERATURE ISING MODEL AT AN EXACT LIMIT

A THESIS

SUBMITTED TO THE DEPARTMENT OF PHYSICS

AND THE INSTITUTE OF ENGINEERING AND SCIENCE

OF BILKENT UNIVERSITY

IN PARTIAL FULFILLMENT OF THE REQUIREMENTS

FOR THE DEGREE OF

MASTER OF SCIENCE

By

Ceyda Sanlı

August, 2008

I certify that I have read this thesis and that in my opinion it is fully adequate, in scope and in quality, as a thesis for the degree of Master of Science.

Prof. Dr. M. Cemal Yalabık (Supervisor)

I certify that I have read this thesis and that in my opinion it is fully adequate, in scope and in quality, as a thesis for the degree of Master of Science.

Prof. Dr. Bilal Tanatar

I certify that I have read this thesis and that in my opinion it is fully adequate, in scope and in quality, as a thesis for the degree of Master of Science.

Prof. Dr. Yiğit Gündüç

Approved for the Institute of Engineering and Science:

Prof. Dr. Mehmet B. Baray
Director of the Institute Engineering and Science

ABSTRACT

TWO-TEMPERATURE ISING MODEL AT AN EXACT LIMIT

Ceyda Sanlı
M.S. in Physics
Supervisor: Prof. Dr. M. Cemal Yalabık
August, 2008

We analyze the order-disorder transition for a two dimensional Ising model. We consider a ferromagnetic exchange interaction between the nearest neighbor Ising spins. The spin exchanges are introduced in two different temperatures, at infinite and finite temperatures. The model is first proposed by Præstgaard, Schmittmann, and Zia [1]. In this thesis, we look at a limit of the system where the spin exchange at infinite temperature proceeds at a very fast rate in one of the lattice direction (the "$y-$direction"). In the other direction (the "$x-$direction"), the spin exchange at a finite temperature is driven by one of several possible exchange dynamics such as Metropolis, Glauber, and exponential rates. We investigate an exact nonequilibrium stationary state solution of the model far from equilibrium. We apply basic stochastic formalisms such as the Master equation and the Fokker-Planck equation. Our main interest is to analyze the possibility of various types of phase transitions.

Using the magnetization as a phase order parameter, we observe two kinds of phase transitions: transverse segregation and longitudinal segregation with respect to the direction x. We find analytically the transition temperature and the nonequilibrium stationary state for small magnetizations at an exact limit. We show that depending on the type of microscopic interaction (such as Metropolis, Glauber, exponential spin exchange rates) the transition temperature and the phase boundary vary. For some exchange rates, we observe no transverse segregation.

Keywords: Nonequilibrium stationary state, the Ising model, the Fokker-Planck equation, phase transition, critical temperature, magnetization.

ÖZET

İKİ SICAKLIKLI ISING MODELİN KESİN BİR SINIR DEĞERİNDEKİ ÇÖZÜMÜ

Ceyda Sanlı
Fizik , Yüksek Lisans
Tez Yöneticisi: Prof. Dr. M. Cemal Yalabık
Ağustos, 2008

Bu tezde, iki boyutlu eşyönlü Ising spin örgüsünde, düzenli fazdan düzensiz faza geçişi inceledik. En yakın komşu spinler arasında ferromanyetik değiş tokuş etkileşimini temel aldık. Problemimizde, spinler arasındaki değiş tokuş sonlu ve sonsuz sıcaklıklar olarak iki farklı sıcaklık altında gerçekleşmektedir. Çalıştığımız model ilk olarak Præstgaard, Schmittmann, ve Zia [1] tarafından önerilmiştir. Verilen modelden farklı olarak biz sonsuz sıcaklık altında yapılan spin değiş tokuşunun diğerine göre çok hızlı olduğu bir sınır değerini incelemekteyiz. Çok hızlı olan bu değiş tokuş örgünün tek bir yönünde (y yönü) gerçekleşmektedir. Diğer yönde ise (x yönü) sonlu sıcaklık altında değiş tokuş yapılmaktadır. Bu yöndeki değiş tokuşu Metroplis, Glauber ve üssel değiş tokuş oranlarıyla incelemekteyiz. Sistemimizin denge durumundan uzak bir noktadaki denge dışı durağan durumunu, kesin bir sınır değerinde araştırmaktayız. Bu amaçla, Master denklemi ve Fokker-Planck denklemi gibi iki temel olasılık yöntemine başvurmaktayız. Çözümlemek istediğimiz asıl nokta sistemde oluşacak olası faz dönüşümleridir. Manyetizasyon değerini faz dönüşüm değişkeni olarak kullandığımızda iki farklı faz dönüşümü gözlemledik. İki faz dönüşümü de ayrılma yapısına uygun faz dönüşümleriydi. Bu dönüşümleri, x doğrultusuna göre enlemesine ayrılma ve boylamasına ayrılma olarak adlandırdık. Faz dönüşümünün gerçekleştiği kritik sıcaklığı ve denge dışı durağan durumu küçük manyetizasyon değerleri için analitik olarak elde ettik. Mikroskopik etkileşmeye bağlı olarak (Problemdeki mikroskopik etkileşim Metropolis, Glauber, ve üssel spin değiş tokuş oranlarıdır.) kritik sıcaklığın ve faz eğrilerinin değişik sonuçlar verdigini gördük. Bazı durumlarda, enlemsel ayrılma gözlemleyemedik.

Anahtar sözcükler: Denge dışı durağan durum, Ising modeli, Fokker-Planck denklemi, faz dönüşümü, kritik sıcaklık, manyetizasyon.

Mustafa'ya, Deniz'e ve Seval'e.

Acknowledgement

I would like to express my gratitude to Prof. Dr. M. Cemal Yalabık. I am really impressed by his curiosity about science. He has taught me to enjoy doing physics that I always remember at the rest of my academic study.

I am thankful to Assoc. Prof. Ceyhun Bulutay, Assoc. Prof. M. Özgür Oktel, Assoc. Prof. F. Ömer İlday, Assoc. Prof. Vikram Tripathi, and Prof. Dr. Ashok Chaterjee for their exciting physics lectures that I have learned a lot.

I am also indebted to Prof. Dr. Bilal Tanatar and Prof. Dr. Yiğit Gündüç for showing keen interest to the subject matter and accepting to read and review this thesis.

I would like to thank to M.Sc. Deniz Çakır, M.Sc. Seval Şener, M.Sc. Arindam Mazumdar, M.Sc. Sandipan Kundu, Dr. Soma Mukhopadyay, and my family members Mr. Mustafa Sanlı, Mr. Ali Nadir Sanlı, and Mrs. Sevim Kırgezen for their morale supports and nice discussions.

Contents

List of Figures

List of Tables

Chapter 1

INTRODUCTION

1.1 Nonequilibrium Physics

Equilibrium statistical mechanics is a well established theory based on Gibbs statistics. The ensemble theory of the equilibrium statistics is considered when the state of an each particle in the system is consistent with the macroscopic condition of the ensemble. However, it is not possible to describe a system by the Gibbs state if any kind of physical flow (particle, energy, probability, *etc.*) does not decay to zero. In this case, the system equilibrium state is no longer valid. Instead, the system may tend to a "nonequilibrium stationary state", for which the equilibrium physics is inadequate. These kind of systems form a very large group in nature and describe various important physical events.

There are numerous research topics which wait to be investigated in nonequilibrium physics. Rheology, granular matter, biological and chemical pattern formations, chemical reaction-diffusion systems and spreading processes are example of nonequilibrium systems which we want to consider very briefly. Even though rheology is a comparable theory with the dense equilibrium systems in some sense, the stress calculations have indicated that some thermodynamic interactions among particles drive the formation of the microstructure which appears only at far-from-equilibrium [2]. Granular flows show phases such as glassy,

frozen, and fluid which can be explained by the dissipative equations [3]. Self-assembly and self-organization have been studied to investigate dissipative chemical and biological formations. In molecular self-assembly, molecules or parts of molecules spontaneously aggregate without any direct human effect [4]. This is important since it appears in essential biological events such as protein folding, structured nucleic acids and technological applications like constructing new chemical nano-meso materials. Self-organization concepts in the cell biology is also significant to understand dynamical cell formations. It has been investigated that many life forms are driven by various physical constraints and collective behaviors which are not under the direct control of the genome [5]. These chemical and biological formations have also been studied by the chemical-reaction diffusion equations [6, 7] which are stochastic theoretical modeling of the thermal diffusion in such dissipative events. The Turing instability is the special name of the successful theoretical model in chemical-reaction diffusion systems to explain such formations [8]. The Turing pattern formations were observed in the nonequilibrium chemical structures [9] and it has been studied to investigate the formation in biological cells [5]. Spatiotemporal chaos (a large number of chaotic elements distributed in space [10]) is the other interesting feature of the nonequilibrium patterns which has not been theoretically developed yet. Spreading problems such as directed percolation to model spreads and recovery of diseases and damage spreads which represents the temporal evaluation of a perturbation (to understand chaotic behavior of the Ising systems) are important issues in the literature to consider nonequilibrium phenomena [7, 11].

There are also some applications of nonequilibrium systems in the condensed matter. Nonequilibrium spin transport in a metal coated with a ferromagnetic film is one of the pioneers work in spintronics [12]. Nonequilibrium spin transport is also used in the superconductor-metal heterostructures [13]. It is indicated that the out-of-equilibrium electrons constructs supercurrent flowing through the heterostructures which is used in magnetic cooling [14]. The segregation in certain molecules observed in organic photovoltaic devices is the other effect of the nonequilibrium spins accumulated in the organic thin films [15]. Self-organization, which was mentioned in the previous paragraph, in organic liquid crystals is also

used in organic photovoltaic thin films [15]. The possible formations in the organic thin films and some other condensed matter structures are summarized briefly in Ref. [16].

So far, we have mentioned briefly some studies which incorporate important nonequilibrium phenomena. Even though these topics have been investigated for more than two decades, there is no unique theory to explain all observations, which makes nonequilibrium physics exciting. The studies also show very rich phase transitions, such that some of the transition properties are defined by the universality classes (See Ref. [7, 11]). In equilibrium, the universality classes show that the dynamics of a system near a critical point (the point where a system exhibits different macroscopic behavior) depend only on its macroscopic properties and they are independent of many of the microscopic details [17]. On the contrary to the equilibrium case, the macroscopic properties of nonequilibrium systems near a critical point may be dependent on the details of the microscopic dynamics [17, 18, 19] which we want to analyze in this thesis for the two dimensional ferromagnetic Ising model.

In the next section, we give some important results in the equilibrium Ising model for better understanding. In the last section, we mention a few pioneers work which help us to visualize our problem.

1.2 Two dimensional Ising model in equilibrium

Collective behavior of the Ising spins in various lattice environments has been of major interest. At a certain temperature, the Ising spins undergo a continuous phase transition from the ferromagnetic state to the paramagnetic state (order to disorder) in equilibrium. In the absence of any external field, spontaneous symmetry breaking occurs as the spins acquire some average magnetization $\langle S \rangle = \pm M_\circ$. The possibility of a phase transition was first predicted by Peierls [20]. He asserted that a spontaneous magnetization may occur at the temperatures lower than a critical value T_c which is responsible to the transition at two dimensional

Ising lattices on the contrary to the 1D Ising chain [21](T_c=0 for the Ising chain). A lot of improvement is proceeded after Onsager solved two dimensional ferromagnetic Ising square lattice exactly in equilibrium in the absence of any external field [22]. He gave the exact critical temperature K_c (K_c=J/k_BT_c where k_B is the Boltzmann constant and T_c is the physical critical temperature) for two dimensional infinite Ising lattice as K_c=0.440.. which is called the Onsager temperature. He also gave the form of the specific heat with the sharp peak around K_c. Later, Yang gave the form of the spontaneous magnetization $M_\circ(T)$ and its shape with respect to the reduced temperature (T/T_c where T_c is the Onsager temperature) by using the transfer matrix method [23]. (See Fig. 1.2. Here, The form of $M_\circ(T)$ is given as $M_\circ(T)$=$\left[\frac{1+x^2}{(1-x^2)^2}(1-6x^2+x^4)^{\frac{1}{2}}\right]^{\frac{1}{4}}$, where x=e^{-2H} and H is a kind of ferromagnetic exchange interaction Hamiltonian.)

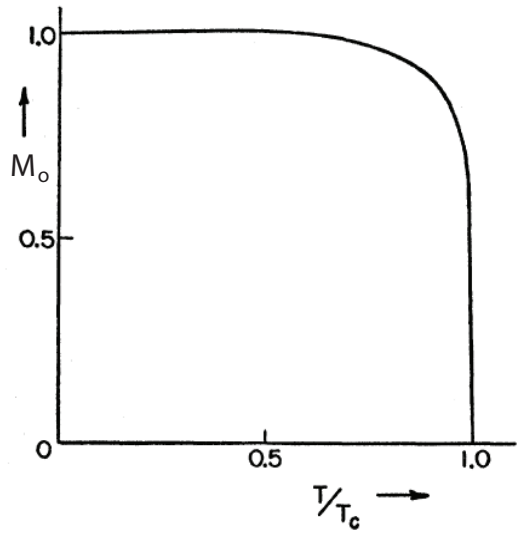

Figure 1.1: Spontaneous magnetization $M_\circ$ versus reduced temperature T/T_c.

The model has been extensively studied by developing new techniques such as the Renormalization Group [24], the Monte Carlo Renormalization Group [25] and the Monte Carlo [26] methods. The universal properties of the model has been obtained by the Renormalization Group method and classified as the Ising universality class [27]. Fig. 1.2 also shows the experimental realization of the

universal property of the magnetization behaves $H/(1-T/T_c)^{\beta+\gamma}$ where H is the magnetic field and β and γ are the critical exponent (The figure is taken from Ref. [28]. Here, the solid curve is given by the three dimensional Heisenberg model where β and γ are equal to 0.3 and 1.4 [29].)

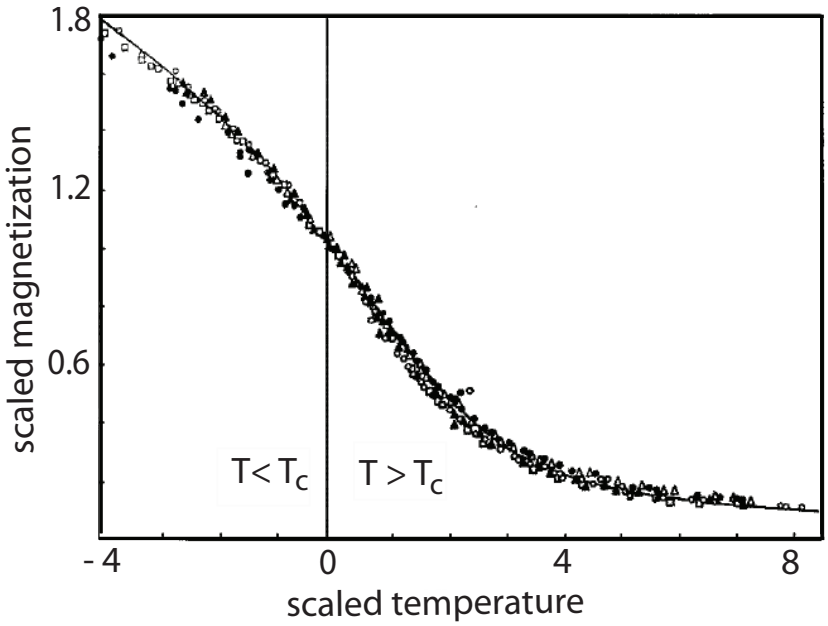

Figure 1.2: The experimental data of the magnetization for five elements showing the universal behavior: The data of $CrBr_3$ (lattice anisotropy), EuO (second-neighbor interactions), Ni (itinerant-electron ferromagnet), YIG (ferrimagnet), and Pd_3Fe (ferromagnetic alloy). All data are consistent with the scaled function given by three dimensional Heisenberg model.

1.3 Two Temperature Ising Model

In this thesis, we investigate the variation in some macroscopic properties of a two dimensional ferromagnetic Ising model depending on the microscopic exchange rates. We investigate the phase behavior of the system for each type of microscopic rates such as Metropolis [30], Glauber [31], and exponential [32] when the system reaches the stationary state . With the aim of studying this, we consider "two temperature Ising model". Two temperature Ising model is one of the

possible nonequilibrium versions of the model solved by Onsager.

Considering nonequilibrium stationary state, two types of the model exist in the literature. One of them is a system with two reservoirs at different finite temperatures. The system is called by the Ising model with "locally competing temperatures". Garrido, Labarta, and Marro [33] investigated two dimensional version of such a system with Glauber spin flip by using the mean field approximation and Metropolis spin flip by the Monte Carlo study. They showed some variations in their mean field and Monte Carlo results. They asserted that the variations are because of the use of different dynamics. Marques [34] applied the mean field renormalization group method to two and three dimensional Ising models with locally competing temperatures with Metropolis spin flip. She gave the critical values and her results were consistent with the equilibrium case (which is a case when two temperatures are equal). Tom*é*, Oliveira, and Santos [35] modified the system given in Ref. [33] by changing one of the bath temperature from positive to negative. By using the mean field renormalization group method, they gave the phase behaviors and the universality properties which were consistent with the equilibrium results. Tamayo, Alexander, and Gupta [36] performed the comparative Monte Carlo study of the spin flip in two dimensional Ising lattice with locally competing temperatures considering dynamics Metropolis, Glauber, and Swendsen-Wang [37]. They found that some of the dynamics gave same universal properties as the equilibrium case.

The other two temperature Ising model is studied when one of the bath is at infinite temperature. The model is mostly used for lattice-gas models which are equivalent to the Ising spin models. In lattice-gas models, particles and holes are represented by $+1$ and 0 on the contrary to the Ising spins ± 1. The two temperature models with infinite bath was first introduced by Garrido, Lebowitz, Maes, and Spohn [38]. They extensively studied correlation functions for an arbitrary microscopic exchange rates. In a time rescaling limit introduced by Masi, Ferrari, and Lebowitz [6], the model is equivalent to the system predicted by Beijeren and Schulman [32]. They considered a lattice-gas which is driven by infinite field in one of the lattice direction so that the spins along that direction become randomized. They investigated the nonequilibrium stationary state and the critical

temperature at an exact limit. Leung, Schmittmann, and Zia [39] studied this model for a finite field with an antiferromagnetic interaction. They gave the behavior of the temperature with respect to the external electric field by the Monte Carlo study and showed the phase behavior. Præstgaard, Schmittmann, and Zia [1] investigated a lattice gas with attractive interaction and in contact with two temperatures. They considered one of the temperatures as infinite along one of the lattice direction so that particle jumps randomly to the nearest neighbor cite if it is empty. In the other direction, they studied the particle exchange driven by Metropolis rate using the Monte Carlo method. They gave the magnetization curve and the critical temperature as $K_c \sim 0.321(2)$ which is the higher than the Onsager value as indicated in Ref. [32]. This model should be consistent with the model introduced in Ref. [32] when the "fast rate" limit [6] is considered. In the fast limit, one of the rate is assumed to be so much larger than the rate in the other direction.

In this thesis, we consider the model introduced in Ref. [1] with the fast rate limit in along the "$y-$direction" corresponding to infinite temperature. In the other direction, we use one of the exchange rates such as Metropolis, Glauber, and the exponential. We investigate the model at an exact stationary limit.

Chapter 2

THEORY

2.1 The Model

We study a model introduced by Præstgaard, Schmittmann, and Zia [1] which contains the randomizing process described in Ref. [6]. They study a two dimensional ferromagnetic Ising model on a square lattice in the absence of any external field with the energy

$$E = -J \sum_{\langle ij \rangle} S_i S_j, \tag{2.1}$$

where J is the coupling constant, S_i and S_j are the Ising lattice spins taking values either ± 1, and $\langle ij \rangle$ represents the nearest neighbor pairs. They have two heat reservoirs with which the lattice contacts: Infinite and finite temperature reservoirs. They are interested in the effect of different spin exchange dynamics in x and y directions. The exchange in the $y-$direction is carried out with a dynamics corresponding to an infinite temperature with a rate ω_y. In the $x-$direction, a finite temperature T is considered so that the exchange is controlled by a mechanism satisfying the detailed balance condition for the transition rate ω_x such that

$$\frac{\omega_x[S_A \leftrightarrow S_B]}{\omega_x[S_B \leftrightarrow S_A]} = e^{H(S_A,S_B)-H(S_B,S_A)}, \tag{2.2}$$

where $H(S_A, S_B)$ is the part of the scaled Hamiltonian described in Eq.(2.1) for the nearest neighbor exchange $S_A \leftrightarrow S_B$. It may be written as

$$H(S_A, S_B) = K\big[S_A(S_1 + S_2 + S_3) + S_B(S_4 + S_5 + S_6)\big], \tag{2.3}$$

where $K = J/k_BT$ and $S_1 \cdots S_6$ are the nearest neighbor spins of S_A and S_B (See Figure 2.1). Præstgaard, Schmittmann, and Zia carry out a Monte Carlo study

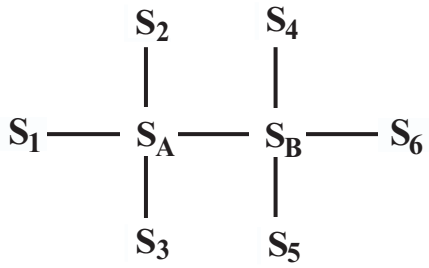

Figure 2.1: Spin configuration of the model: Spins used in $H(S_A, S_B)$ are shown.

of this model with Metropolis exchanges in both directions. They report results including a phase transition at a temperature 40% higher than the equilibrium model ($K_c \sim 0.321(2)$). This is an interesting result in that in spite of the disorder-increasing effect of the infinite temperature, the system reaches order a higher temperature of the finite temperature bath, in comparison to the equilibrium temperature.

In our work, we consider an infinitely fast dynamics corresponding to the exchange at infinite temperature. The model we introduce is equivalent to the model given by Beijeren and Schulman [32]. They consider infinitely driven lattice gas along one of the lattice direction (the "$y-$direction") where the jump rate can be assumed to be so larger than the rate of the other direction. So, the spins along the $y-$direction become randomized. They investigate the nonequilibrium stationary state of the system for a specific jump rate along $x-$direction which we call as exponential rate. In our case, similarly spins $S_1 \cdots S_6$ are randomized due to the selection of a very fast exchange rate ω_y compared to ω_x. Since we take $\omega_y \gg \omega_x$, the values of spins at lattice sites with a certain $x-$coordinate may be

assumed to be random along $y-$direction with some magnetization $m(x)$. So, we can assume that spins at each column are independent of the other column's when the time difference between two exchanges in $y-$direction (t_y) is infinitely smaller than the time difference between two exchanges in $x-$direction (t_x) (*i.e.* $t_y \ll t_x$). However, the exchange process in $x-$direction (driven by ω_x) changes the magnitude of $m(x)$. Thus, the probability function of such spins for a spin variable S with lattice coordinate x is given by

$$\rho(S,x) = \frac{1 + m(x)\, S}{2}, \tag{2.4}$$

where $m(x) = 2n(x)/N - 1$. Here, $n(x)$ is the number of plus spins with coordinate x and N is the number of total spins with that $x-$coordinate. Note that we will also treat $n(x)$ as a random variable. We study three types of exchange mechanism: Metropolis, Glauber, and exponential which satisfy the condition defined in Eq.(2.2). The form of rate ω_x depending on these mechanisms is described as follows

$$\omega_x[H(S_A,S_B)] = \begin{cases} \alpha \min[1, e^{-2H(S_A,S_B)}] & \text{Metropolis,} \\ \alpha[1 - \tanh(H(S_A,S_B))] & \text{Glauber,} \\ \alpha e^{-H(S_A,S_B)} & \text{exponential,} \end{cases} \tag{2.5}$$

where α is a constant which sets the time-scale. The exchange rate for exchanging spin S at coordinate x with the nearest neighbor spin $-S$ at $x \pm 1$ is

$$\bar{\omega}(S,\, n(x),\, x,\, x \pm 1) = \rho(S,x)\rho(-S, x \pm 1) \tag{2.6}$$
$$\times \Big(\sum_{S_1 \cdots S_6} \rho(S_1, x \mp 1)\rho(S_2,x)\rho(S_3,x)\rho(S_4, x \pm 1)\rho(S_5, x \pm 1)\rho(S_6, x \pm 2)\omega_x[H(S,-S)] \Big).$$

In the following section, we will derive the master equation for the model presented here.

2.2 The Master Equation

In this thesis, we are interested in the variation of the magnetization along the lattice. In the limit of $\omega_y \gg \omega_x$, *i.e.* $t_y \ll t_x$, the magnetization along each column is represented by the random quantity $m(x)$ and the spin probability density corresponding to this $m(x)$ is equivalent to

$$\rho(S, x) = \frac{1 + m(x)\, S}{2}. \tag{2.7}$$

Owing to the effect of the nearest neighbor interactions, the spin probability flow is driven by the rate $\bar{\omega}$ as defined at Eq. 2.6. So, the spin probability density has diffusive character and the probability flow makes the system to be far-from-equilibrium. In this section, we will consider this nonequilibrium behavior.

We apply the Master equation formalism to investigate the spin probability density due to $\bar{\omega}$. Figure 2.2 represents the possible exchanges between two spins S_A and S_B. The nearest neighbors are considered as the interaction energy given in Eq. 2.3.

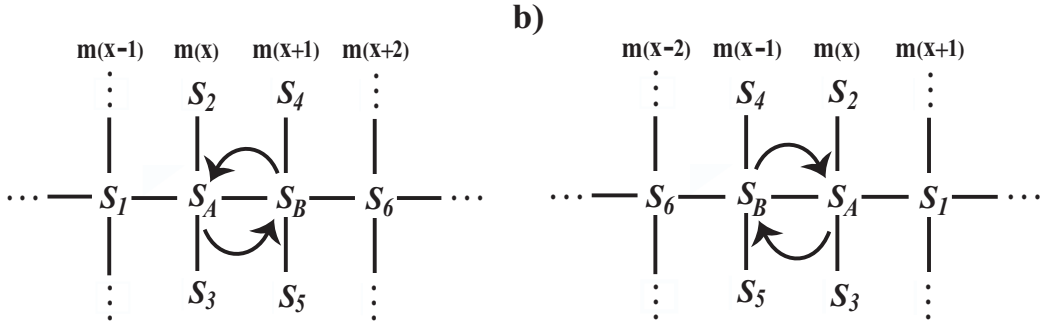

Figure 2.2: The nearest neighbor spin exchanges: There are two directions for the nearest neighbor spin exchanges. Due to Eq. 2.6, the exchange direction right (a) is driven by $\bar{\omega}(S,\, n(x),\, x,\, x+1)$ and the direction left (b) is driven by $\bar{\omega}(S,\, n(x),\, x,\, x-1)$.

In general, the master equation for the probability density of S_A is defined as

$$\frac{\partial}{\partial t}P(S_A, n(x)) = -P(S_A, n(x))\,\bar{\omega}(S_A \longrightarrow S_B) + P(S_B, n(x) \pm 1)\,\bar{\omega}(S_B \longrightarrow S_A), \qquad (2.8)$$

where $P(S_A, n(x))$ and $P(S_B, n(x) \pm 1)$ are the nonequilibrium spin probability densities. The exchange is significant only if $S_A = -S_B$. So, for any exchanged spin S_A at the column with magnetization $m(x)$, $n(x)$ either decreases or increases so that $P(S_A, n(x))$ decreases. If $S_B = +1$ and the number of plus spin at x is equal to $n(x) - 1$, the process increases $P(S_A, n(x))$. Similarly, if $S_B = -1$ and the number of plus spin at x is equal to $n(x) + 1$, the process also increases $P(S_A, n(x))$. Thus, the master equation corresponding to the rate $\bar{\omega}$ can be interpreted as follows:

$$\begin{aligned}\frac{\partial}{\partial t}P(n(x), x) = &- P(n(x), x) \sum_{S=\pm 1} \big[\bar{\omega}(S,\, n(x),\, x,\, x+1) + \bar{\omega}(S,\, n(x),\, x,\, x-1)\big] \\ &+ P(n(x)-1, x)\big[\bar{\omega}(-1,\, n(x)-1,\, x,\, x+1) + \bar{\omega}(-1,\, n(x)-1,\, x,\, x-1)\big] \\ &+ P(n(x)+1, x)\big[\bar{\omega}(+1,\, n(x)+1,\, x,\, x+1) + \bar{\omega}(+1,\, n(x)+1,\, x,\, x-1)\big],\end{aligned} \qquad (2.9)$$

where $P(n(x), x)$ is the nonequilibrium probability density at coordinate x with a certain $n(x)$, and the time dependence is implicit. We are interested in the nonequilibrium stationary state solution of Eq.(2.9) where $\frac{\partial}{\partial t}P(n(x), x) = 0$.

2.3 The Fokker-Planck Equation

The master equation we have derived is called as the microscopic Markovian master equation [40]. We are interested in the possible analytic solution of the nonequilibrium probability density. So, we need to obtain the differential form of Eq. 2.9. In the macroscopic limit, $N \gg 1$ can be considered such that $m(x)$ becomes a continuous variable of $n(x)$. In Eq. 2.9, we have discrete quantities *i.e.* $n(x) + 1$ and $n(x) - 1$. For large N, these quantities correspond to $m(x) + \Delta m$ and $m(x) - \Delta m$, respectively where $\Delta m = 2/N$ so that Eq. 2.9 can be written

as

$$\frac{\partial}{\partial t}P(m(x),x) = -P(m(x),x)\sum_{S=\pm 1}\big[\bar{\omega}(S,\, m(x),\, x,\, x+1) + \bar{\omega}(S,\, m(x),\, x,\, x-1)\big] \tag{2.10}$$

$$+ P(m(x)-\Delta m, x)\big[\bar{\omega}(-1,\, m(x)-\Delta m,\, x,\, x+1) + \bar{\omega}(-1,\, m(x)-\Delta m,\, x,\, x-1)\big]$$

$$+ P(m(x)+\Delta m, x)\big[\bar{\omega}(+1,\, m(x)+\Delta m,\, x,\, x+1) + \bar{\omega}(+1,\, m(x)+\Delta m,\, x,\, x-1)\big],$$

where P and $\bar{\omega}$'s can be expanded with respect to the small quantity Δm. Considering the expansion up to $(\Delta m)^2$, we have

$$\frac{\partial}{\partial t}P(m(x),x) = -P(m(x),x)\sum_{S=\pm 1}\big[\bar{\omega}(S,\, m(x),\, x,\, x+1) + \bar{\omega}(S,\, m(x),\, x,\, x-1)\big] \tag{2.11}$$

$$+ P(m(x),x)\big[\bar{\omega}(-1,\, m(x),\, x,\, x+1) + \bar{\omega}(-1,\, m(x),\, x,\, x-1)\big]$$

$$- \Delta m\,\frac{\partial}{\partial m}\Big(P(m(x),x)\big[\bar{\omega}(-1,\, m(x),\, x,\, x+1) + \bar{\omega}(-1,\, m(x),\, x,\, x-1)\big]\Big)$$

$$+ \frac{(\Delta m)^2}{2}\,\frac{\partial^2}{\partial m^2}\Big(P(m(x),x)\big[\bar{\omega}(-1,\, m(x),\, x,\, x+1) + \bar{\omega}(-1,\, m(x),\, x,\, x-1)\big]\Big)$$

$$+ P(m(x),x)\big[\bar{\omega}(+1,\, m(x),\, x,\, x+1) + \bar{\omega}(+1,\, m(x),\, x,\, x-1)\big]$$

$$+ \Delta m\,\frac{\partial}{\partial m}\Big(P(m(x),x)\big[\bar{\omega}(+1,\, m(x),\, x,\, x+1) + \bar{\omega}(+1,\, m(x),\, x,\, x-1)\big]\Big)$$

$$+ \frac{(\Delta m)^2}{2}\,\frac{\partial^2}{\partial m^2}\Big(P(m(x),x)\big[\bar{\omega}(+1,\, m(x),\, x,\, x+1) + \bar{\omega}(+1,\, m(x),\, x,\, x-1)\big]\Big).$$

The following notations simplify Eq. 2.11:

$$\begin{aligned}\bar{\omega}_+(m) &= \bar{\omega}(+1,\, m(x),\, x,\, x+1) + \bar{\omega}(+1,\, m(x),\, x,\, x-1), \\ \bar{\omega}_-(m) &= \bar{\omega}(-1,\, m(x),\, x,\, x+1) + \bar{\omega}(-1,\, m(x),\, x,\, x-1),\end{aligned} \tag{2.12}$$

where the dependence of $\bar{\omega}_+$ and $\bar{\omega}_-$ on $m(x)$ is now implicit. Using Eq. 2.12 in Eq. 2.11 we have

$$\frac{\partial}{\partial t}P(m,x) = \frac{(\Delta m)^2}{2}\frac{\partial^2}{\partial m^2}\Big(\big[\,\bar{\omega}_+(m) + \bar{\omega}_-(m)\,\big]P(m,x)\Big) \tag{2.13}$$

$$+\,\Delta m\frac{\partial}{\partial m}\Big(\big[\,\bar{\omega}_+(m) - \bar{\omega}_-(m)\,\big]P(m,x)\Big),$$

where we use the shorthand notation $m = m(x)$. This is the Fokker-Planck equation of the nonequilibrium spin probability density $P(m,x)$ [17, 40]. In this thesis, we consider $P(m,x)$ to investigate the critical behavior of the spins satisfying Eq.(2.13). In the next chapter, we will discuss the phase transition behavior of Eq.(2.13) for three distinct types of exchange mechanism ω_x given in Eq.(2.5). In the following section, we will provide some algebra which will be necessary in the next chapter.

2.4 Rate Analysis

In the literature, a number of exchange dynamics are commonly used in the critical phenomena of the Ising model. In this thesis, we will consider three types of mechanisms: Metropolis, Glauber, and exponential. These three rates satisfy the detailed balance condition defined in Eq.(2.2). The detailed balance condition is an important restriction for transition rates of the equilibrium Ising model. Even though it is not compulsory, this condition is frequently used for nonequilibrium problems which eventually reach an equilibrium state represented as the Gibbs state.

Let us consider ω_x defined as follows:

$$\omega_x[H(S,-S)] = \begin{cases} \alpha\min[1, e^{-2H(S,-S)}] & \text{Metropolis,} \\ \alpha[1-\tanh(H(S,-S))] & \text{Glauber,} \\ \alpha e^{-H(S,-S)} & \text{exponential.} \end{cases} \tag{2.14}$$

where $H(S,-S) = K\ S(S_1+S_2+S_3-S_4-S_5-S_6)$. For attractive interaction (ferromagnetic case), $K > 0$. Here, we discuss an expansion of ω_x which help to simplify our calculations to evaluate Eq.(2.13). We can define ω_x in terms of $S_1 \cdots S_6$ such that

$$\begin{aligned}\omega_x = \quad & a_0 + a_1(S_1+S_2+S_3-S_4-S_5-S_6) + a_2(S_1S_2+\cdots+S_5S_6) \\ & + a_3(S_1S_2S_3+\cdots-S_4S_5S_6) + a_4(-S_1S_2S_3S_4+\cdots-S_3S_4S_5S_6) \\ & + a_5(S_1S_2S_3S_4S_5+\cdots-S_2S_3S_4S_5S_6) + a_6(-S_1S_2S_3S_4S_5S_6),\end{aligned} \tag{2.15}$$

where a_0, a_1, a_2, a_3, a_4, a_5, and a_6 are the expansion coefficients of ω_x in terms of the spin products. The quantities $a_0 \cdots a_6$ are defined by the equality

$$a_i = \frac{1}{2^6} \sum_{S_1 \cdots S_6} \Big(\prod_{j \text{ spins}} S_\beta \prod_{|i-j| \text{ spins}} S_\gamma\ \omega_x\{S\} \Big). \tag{2.16}$$

Here, S_β is one of S_1, S_2, S_3 and S_γ is one of $-S_4$, $-S_5$, $-S_6$. We will give the expressions of $a_0 \cdots a_3$ as an example.

$$\begin{aligned}
a_0 &= \frac{1}{2^6} \sum_{S_1 \cdots S_6} \omega_x\{S\}, \qquad (2.17)\\
a_1 &= \frac{1}{2^6} \sum_{S_1 \cdots S_6} S_\beta\, \omega_x\{S\} = \frac{1}{2^6} \sum_{S_1 \cdots S_6} (-S_\gamma)\, \omega_x\{S\}, \\
a_2 &= \frac{1}{2^6} \sum_{S_1 \cdots S_6} S_\beta\, S_{\beta'}\, \omega_x\{S\} = \frac{1}{2^6} \sum_{S_1 \cdots S_6} S_\gamma\, S_{\gamma'}\, \omega_x\{S\} = \frac{1}{2^6} \sum_{S_1 \cdots S_6} (-S_\beta\, S_\gamma)\, \omega_x\,\{S\}, \\
a_3 &= \frac{1}{2^6} \sum_{S_1 \cdots S_6} S_\beta\, S_{\beta'}\, S_{\beta''}\, \omega_x\{S\} = \frac{1}{2^6} \sum_{S_1 \cdots S_6} (-S_\gamma\, S_{\gamma'}\, S_{\gamma''})\, \omega_x\{S\} \\
&= \frac{1}{2^6} \sum_{S_1 \cdots S_6} S_\beta\, S_\gamma\, S_{\gamma'}\, \omega_x\{S\} = \frac{1}{2^6} \sum_{S_1 \cdots S_6} (-S_\beta\, S_{\beta'}\, S_\gamma)\, \omega_x\{S\}.
\end{aligned}$$

For each type of ω_x, the values of $a_0 \cdots a_6$ are given Table 2.1. We will consider $H(S,-S)$ for $S = +1$ so that for $S = -1$ odd S_γ terms (a_1, a_3, and a_5) should be multiplied by -1 while even S_γ terms (a_0, a_2, a_4, and a_6) stay the same. We want to indicate that the coefficients $a_0 \cdots a_6$ are same for both $\bar{\omega}(S,\, m(x),\, x,\, x+1)$ and $\bar{\omega}(S,\, m(x),\, x,\, x-1)$ which are the right exchange rate shown in Figure 2.2(a) and the left exchange rate shown in Figure 2.2(b), respectively.

Table 2.1: Expansion coefficients of ω_x: $a_0 \cdots a_6$ values are shown for each dynamics with the multiplications by 64 of their original values. Here, r and $t(c\,K)$ stand for exp (-2K) and the tanh $(c\,K)$ function, respectively.

ω_x	Metropolis	Glauber	exponential
a_0	$42 + 15r^2 + 6r^4 + r^6$	64	$20 + 15(r + \frac{1}{r}) + 6(r^2 + \frac{1}{r^2}) + (r^3 + \frac{1}{r^3})$
a_1	$-10 + 5r^2 + 4r^4 + r^6$	$-10\,t(2\mathrm{K}) - 8\,t(4\mathrm{K}) - 2\,t(6\mathrm{K})$	$5(r - \frac{1}{r}) + 4(r^2 - \frac{1}{r^2}) + (r^3 - \frac{1}{r^3})$
a_2	$-2 - r^2 + 2r^4 + r^6$	0	$-4 - (r + \frac{1}{r}) + 2(r^2 + \frac{1}{r^2}) + (r^3 + \frac{1}{r^3})$
a_3	$2 - 3r^2 + r^6$	$6\,t(2\mathrm{K}) - 2\,t(6\mathrm{K})$	$-3(r - \frac{1}{r}) + (r^3 - \frac{1}{r^3})$
a_4	$2 - r^2 - 2r^4 + r^6$	0	$4 - (r + \frac{1}{r}) - 2(r^2 + \frac{1}{r^2}) + (r^3 + \frac{1}{r^3})$
a_5	$-2 + 5r^2 - 4r^4 + r^6$	$-10\,t(2\mathrm{K}) + 8\,t(4\mathrm{K}) - 2\,t(6\mathrm{K})$	$5(r - \frac{1}{r}) - 4(r^2 - \frac{1}{r^2}) + (r^3 - \frac{1}{r^3})$
a_6	$-10 + 15r^2 - 6r^4 + r^6$	0	$-20 + 15(r + \frac{1}{r}) - 6(r^2 + \frac{1}{r^2}) + (r^3 + \frac{1}{r^3})$

Chapter 3

RESULTS

In this chapter, we focus on the possible solution(s) of the Fokker-Planck equation which we have derived in the previous section. Let us recall Eq.(2.13) as follows:

$$\frac{\partial}{\partial t}P(m,x) = \frac{(\Delta m)^2}{2}\frac{\partial^2}{\partial m^2}\big[\,\bar{\omega}_1(m)\,P(m,x)\,\big] + \Delta m\frac{\partial}{\partial m}\big[\,\bar{\omega}_2(m)\,P(m,x)\,\big]\,, \qquad (3.1)$$

where $\bar{\omega}_1(m)$ and $\bar{\omega}_2(m)$ are

$$\begin{aligned} \bar{\omega}_1(m) &= \bar{\omega}_+(m) + \bar{\omega}_-(m)\,, \\ \bar{\omega}_2(m) &= \bar{\omega}_+(m) - \bar{\omega}_-(m)\,. \end{aligned} \qquad (3.2)$$

Here, we still use implicit m dependence in $\bar{\omega}$'s. For the stationary state case, Eq.(3.1) becomes

$$\Delta m\frac{d}{d\,m}\left(\frac{\Delta m}{2}\frac{d}{d\,m}\big[\bar{\omega}_1(m)\,P(m,x)\big] + \bar{\omega}_2(m)\,P(m,x)\right) = 0. \qquad (3.3)$$

This yields to the following equation

$$\Delta m\,\bar{\omega}_1(m)\,\frac{d}{d\,m}P(m,x) + \Delta m\,P(m,x)\,\frac{d\,\bar{\omega}_1(m)}{d\,m} + P(m,x)\,\bar{\omega}_2(m) = 0. \qquad (3.4)$$

For $N \gg 1$, $\Delta m \ll 1$ so that the second term of Eq.(3.4) can be negligible. So, we have

$$\frac{d\,P(m,x)}{P(m,x)} = -\frac{2}{\Delta m}\,\frac{\bar{\omega}_2(m)}{\bar{\omega}_1(m)}\,d\,m\,, \tag{3.5}$$

which gives the following solution

$$P(m,x) = A\exp\left(-\frac{2}{\Delta m}\int_{-1}^{m} dm\,\frac{\bar{\omega}_2}{\bar{\omega}_1}\right), \tag{3.6}$$

where A is the normalization constant. For small Δm, Eq.(3.6) gives delta function solution(s) with the peak(s) at the maxima of the argument of the exponential. We will call these particular m value(s) where the peak(s) occurred as m_s.

Along the lattice, there is a spontaneous magnetization which is the average quantity over all possible m values such that

$$M(x,t) = \int_{-1}^{1} dm\; m\,P(m,x)\,, \tag{3.7}$$

where $P(m,x)$ is given in Eq.(3.6). The instability in this nonequilibrium spontaneous magnetization is significant for the phase transition which we will investigate the following sections. We will show two kinds of instability depending on spatially invariant and spatially dependent spontaneous magnetization. Both of them will present segregation type phase transition which may be labeled as transverse segregation (transverse to the $x-$coordinate) and longitudinal segregation (longitudinal to the $x-$coordinate), respectively.

3.1 Transverse Segregation

One form of the instability may be the segregation of $+1$ and -1 spins for a particular $x-$coordinate. For stationary state case, let us consider M as spatially invariant along $x-$direction so that $M(x) = M_\circ$ where $M_\circ$ is a constant between -1 and $+1$. P is then independent of x. From Eq.(3.6), we have shown that the steady state probability function $P(m, x)$ has peak(s) at m_s. Besides the case $m_s = M_\circ$, the spins configure themselves at certain K such that m_s starts to be different from $M_\circ$. This K is the critical point (K_c) where the spins segregate to satisfy m_s, with $m_s \neq M_\circ$. We label this collective behavior as transverse segregation (transverse to the $x-$coordinate).

We evaluate m_s and K_c for $M_\circ = 0$ analytically. For a finite $M_\circ$, we apply a graphical solution. Let us first consider the $M_\circ = 0$ case. From Eq.(3.6), m_s may be found from $\bar{\omega}_2/\bar{\omega}_1 = 0$ so that we investigate the condition $\bar{\omega}_2 = 0$. Due to the definition of $\bar{\omega}_2$ given in Eq.(3.2), we should calculate $\bar{\omega}_+$ and $\bar{\omega}_-$. With $M_\circ = 0$, the probability function becomes $\rho(S) = 1/2$ for S_1, S_4, S_5, and S_6. For S_2 and S_3, which are at coordinate x, the form given in Eq.(2.6) must be used to obtain the probabilities corresponding to the random variable m. We then have the following equality:

$$\bar{\omega}_S(m) = \bar{\omega}(S, m, x, x \pm 1), \tag{3.8}$$

where

$$\bar{\omega}_S(m) = \frac{1}{2^5}\,\rho(S, x) \sum_{S_1 \cdots S_6} \rho(S_2, x)\rho(S_3, x)\omega_x[H(S, -S)]. \tag{3.9}$$

So, the condition $\bar{\omega}_2 = 0$ is equivalent to

$$\begin{aligned} \rho(-1, x) \sum_{S_1 \cdots S_6} \rho(S_2, x)\rho(S_3, x)\omega_x[-H(S, -S)] \\ - \rho(+1, x) \sum_{S_1 \cdots S_6} \rho(S_2, x)\rho(S_3, x)\omega_x[H(S, -S)] = 0, \end{aligned} \tag{3.10}$$

which gives a polynomial equation of m such that

$$(1-m)\left(\sum_{S_1\cdots S_6}\omega_x\{S\} - m\sum_{S_1\cdots S_6}(S_2+S_3)\,\omega_x\{S\} + m^2\sum_{S_1\cdots S_6}S_2S_3\,\omega_x\{S\}\right) \tag{3.11}$$
$$-(1+m)\left(\sum_{S_1\cdots S_6}\omega_x\{S\} + m\sum_{S_1\cdots S_6}(S_2+S_3)\,\omega_x\{S\} + m^2\sum_{S_1\cdots S_6}S_2S_3\,\omega_x\{S\}\right) = 0.$$

Using the expansion coefficients $a_0\cdots a_6$ calculated in the previous chapter in Eq.(3.11), we have

$$m(a_0 + 2a_1 + a_2m^2) = 0, \tag{3.12}$$

which yields $m_s = 0$ and the following solution:

$$m_s = \pm\sqrt{-\frac{a_0+2a_1}{a_2}}. \tag{3.13}$$

We calculate m_s and K_c for each ω_x shown in Table 3.1. We find that transverse segregation occurs only for the exponential rate. Figure 3.1 shows the behavior of $\bar{\omega}_2$ with respect to m for some K values and for K_c.

For a finite $M_\circ$, Eq.(3.11) becomes complicated so that the corresponding version of Eq.(3.12) cannot be obtained easily. So, we obtain $\bar{\omega}_2$ with respect to m graphically in the following figure. We again cannot find a phase transition into the transverse segregation for the Metropolis and Glauber rates.

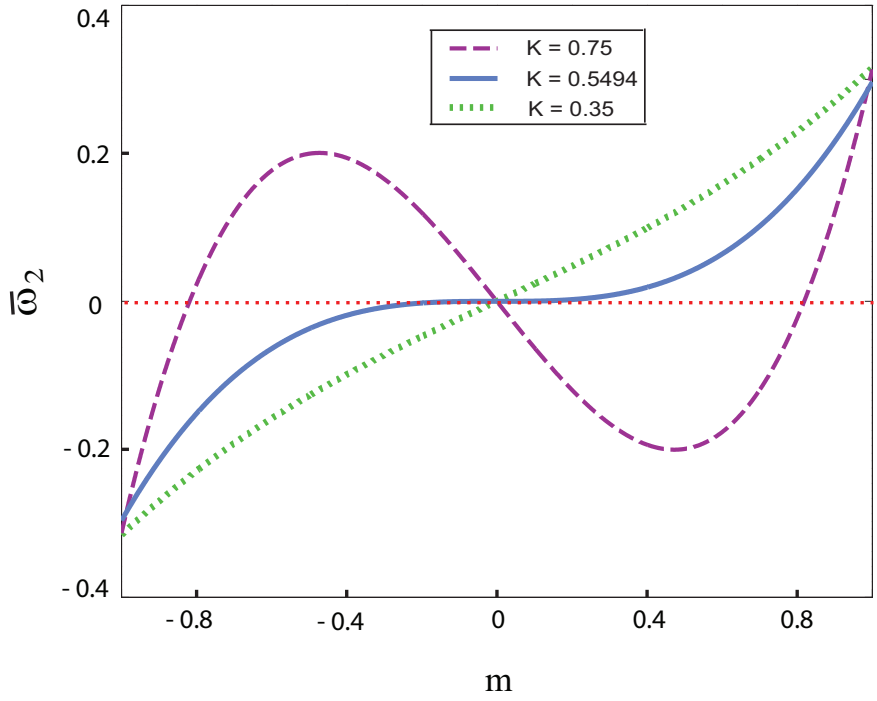

Figure 3.1: The transverse segregation of the exponential rate for $M_\circ = 0$ case: The critical behavior is given by the solid curve as $K_c = 0.5494$. The dashed and the dotted curves are calculated for $K = 0.75$ and $K = 0.35$, respectively.

Table 3.1 summarizes the transverse segregation for each ω_x and for some $M_\circ$.

Table 3.1: m_s and K_c values are represented for the transverse segregation. The values of $M_\circ = 0$ are found exactly.

ω_x	$M = 0$		$M = \pm 0.5$	
	m_s	K_c	m_s	K_c
exponential	± 0.0237	0.5494	$\mp 0.114\,; \mp 0.404$	0.59
Metropolis	none	none	none	none
Glauber	none	none	none	none

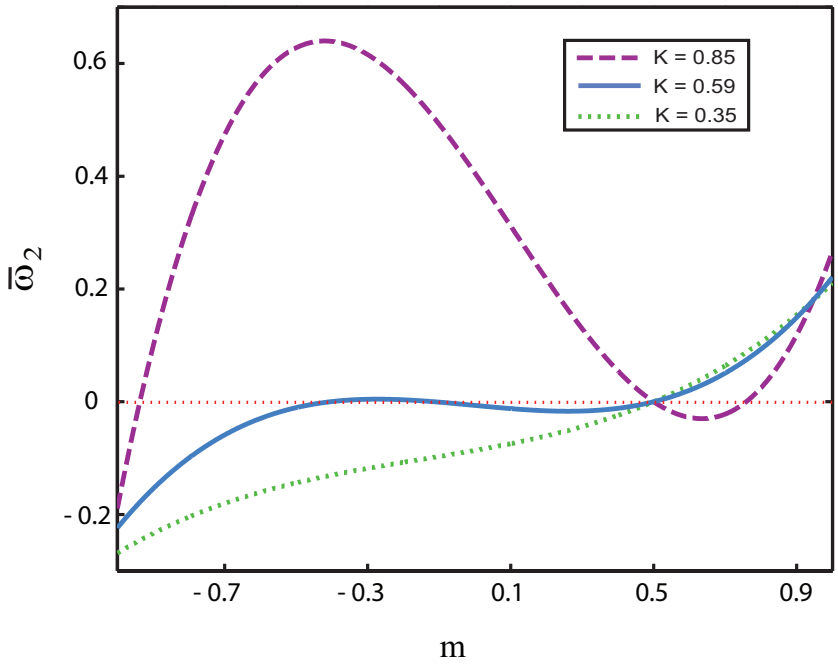

Figure 3.2: The transverse segregation of the exponential rate for $M_\circ = 0.5$ case: The critical behavior is given by the solid curve as $K_c = 0.59$. The dashed and the dotted curves are calculated for $K = 0.85$ and $K = 0.35$, respectively.

3.2 Longitudinal Segregation

Another form of instability occurs at smaller values of K (higher temperatures). This instability is the result of the segregation longitudinally (longitudinal to the $x-$coordinate) so that $M(x) = 0$ is no longer valid. It is evident that the fast randomization process allows only for a $\delta-$function distribution for the probability density as we have discussed at the previous section. Consider then the density $P(m, x) = \delta\big(m - M(x, t)\big)$. Integrating both sides of Eq.(3.1) by $\int_{-1}^{1} dm\, m$ with

the density $\delta\big(m - M(x,t)\big)$ yields

$$\int_{-1}^{1} dm\, m\, \frac{\partial}{\partial t}\delta\big(m - M(x,t)\big) = \Delta m \int_{-1}^{1} dm\, m\, \frac{\partial}{\partial m}\Big[\bar{\omega}_2(m)\, \delta\big(m - M(x,t)\big)\Big] \tag{3.14}$$
$$+ \frac{(\Delta m)^2}{2} \int_{-1}^{1} dm\, m\, \frac{\partial^2}{\partial m^2}\Big[\bar{\omega}_1(m)\, \delta\big(m - M(x,t)\big)\Big],$$

By applying an integration by parts to RHS (right hand side) of Eq.(3.1), and neglecting the $(\Delta m)^2$ term we have

$$\frac{\partial}{\partial t} M(x,t) = -\Delta m\, \bar{\omega}_2\big(M(x,t)\big), \tag{3.15}$$

where

$$\begin{aligned}\bar{\omega}_2\big(M(x,t)\big) =& \bar{\omega}(S=+1, M(x,t), x+1) + \bar{\omega}(S=+1, M(x,t), x-1) \\ &- \bar{\omega}(S=-1, M(x,t), x+1) - \bar{\omega}(S=-1, M(x,t), x-1).\end{aligned} \tag{3.16}$$

For small $M(x,t)$ near a critical point $\bar{\omega}(S, M(x,t), x \pm 1)$ may be expanded in orders of M as

$$\bar{\omega}(S, M(x), x \pm 1) = \frac{1}{2^8}\big(1 - SM(x \pm 1) + SM(x)\big) \times \sum_{S_1 \cdots S_6} \big[\,\big(1 + S_1 M(x \mp 1) \tag{3.17}$$
$$+ S_2 M(x) + S_3 M(x) + S_4 M(x \pm 1) + S_5 M(x \pm 1) + S_6 M(x \mp 2) + o(M^2)\big)\omega_x[H(S,-S)]\,\big],$$

where t dependence has been dropped. Using the definitions of a_0 and a_1 in Eq.(3.17) we have

$$\begin{aligned}\bar{\omega}(S, M(x), x \pm 1) =& \frac{a_0}{4}\big(\,1 - SM(x \pm 1) + SM(x)\,\big) \\ &+ \frac{Sa_1}{4}\big(\,M(x \mp 1) + 2M(x) - 2M(x \pm 1) - M(x \pm 2)\,\big) + o(M^2).\end{aligned} \tag{3.18}$$

For small $M(x,t)$, only the first order terms need to be considered. We have the critical condition $\bar{\omega}_2 = 0$ so that when the following equality becomes zero, the

condition will be satisfied.

$$\begin{aligned}\bar{\omega}_2 =& \frac{a_0}{2}\Big(2M(x) - M(x-1) - M(x+1)\Big) \\ &+ \frac{a_1}{2}\Big(4M(x) - M(x-1) - M(x+1) - M(x-2) - M(x+2)\Big).\end{aligned} \tag{3.19}$$

This form suggests expanding $M(x,t)$ using the Fourier series as

$$M(x,t) = \sum_{\ell} f_\ell(t) \exp(i\, 2\pi \ell\, x/L), \tag{3.20}$$

where ℓ is the wavenumber and L is the lattice length. Fourier transforming Eq.(3.15) we obtain

$$\frac{\partial}{\partial t} f_\ell(t) = \Delta m\Big(\, a_0\,[1 - \cos(2\pi\ell/L)] + a_1\,[2 - \cos(2\pi\ell/L) - \cos(4\pi\ell/L)]\,\Big) f_\ell(t). \tag{3.21}$$

This equation can be simplified by the following trigonometric identity

$$\sin^2(\pi\ell/L) + \sin^2(2\pi\ell/L) = \frac{1}{2}\Big(2 - \cos(2\pi\ell/L) - \cos(4\pi\ell/L)\Big). \tag{3.22}$$

So, Eq.(3.21) yields

$$\frac{\partial}{\partial t} f_\ell(t) = 2\Delta m\,\Big(a_0 + a_1\,[\,4\cos^2(\pi\ell/L) + 1\,]\Big)\sin^2(\pi\ell/L)/2\;\; f_\ell(t). \tag{3.23}$$

Note that the sign of the term in the brackets determines whether the ℓ'th mode grows or decays. Thus, the critical condition is satisfied for the following equality

$$\frac{a_0}{a_1} = -\big[\,4\cos^2(\pi\ell/L) + 1\,\big]. \tag{3.24}$$

Note that a_1 is negative and the ratio $-a_0/a_1$ decreases as the temperature decreases. The highest value on the RHS of Eq.(3.24) then corresponds to the mode which first becomes unstable at a particular K which gives K_c. This occurs for $\ell = 0$ (uniform magnetization) at $a_0/a_1 = -5$. In Table 3.2, we show the different K_c values for each type of ω_x.

These results indicate that we have a higher K_c for longitudinal segregation

Table 3.2: K_c values when $\ell = 0$ for each ω_x.

ω_x	K_c
Metropolis	0.4309
Glauber	0.2590
exponential	0.2028

than transverse one. Note that in principle the transverse segregation could also appear at temperatures lower than the K_c of longitudinal segregation and the two types of order may coexist, although we have not analyzed this possibility in detail. We should note that the exponential rate result corresponding to the fast dynamics case of Ref. [32], where they identify a critical point at 0.2 using the divergence of the susceptibility is not consistent with our result as shown in Table 3.2.

3.3 Shape of Magnetization

The shape of magnetization $M(x)$ for longitudinal segregation can be found if the expansion order shown in Eq.(3.17, 3.18) can be generated such that M^2 and M^3 terms are also considered. In this case, corresponding Eq.(3.23) includes terms such as the term proportional to "$f_\ell\, f_{\ell'}$" and the term proportional to "$f_\ell\, f_{\ell'}\, f_{\ell''}$". Due to the lattice symmetry, the second order term $f_\ell\, f_{\ell'}$ has no contribution so that $f_\ell\, f_{\ell'}\, f_{\ell''}$ term yields to the approximate shape of $M(x)$. However, we could not obtain successful formalism due to the difficulty of combining trigonometric functions in the Fourier transform. So, we apply a numerical methods shown as follows.

We consider Eq.(2.9) with the corresponding quantities of m and $m \pm \Delta m$ for n and $n \pm 1$ such that

$$\begin{aligned}\frac{\partial}{\partial t}P(m,x) = &- P(m,x) \sum_{S=\pm 1} \big[\bar{\omega}(S,\, m,\, x,\, x+1) + \bar{\omega}(S,\, m,\, x,\, x-1)\big] \\ &+ P(m-\Delta m,x)\big[\bar{\omega}(-1,\, m-\Delta m,\, x,\, x+1) + \bar{\omega}(-1,\, m-\Delta m,\, x,\, x-1)\big] \\ &+ P(m+\Delta m,x)\big[\bar{\omega}(+1,\, m+\Delta m,\, x,\, x+1) + \bar{\omega}(+1,\, m+\Delta m,\, x,\, x-1)\big].\end{aligned} \tag{3.25}$$

Using $P(m,x) = \delta\big(m - M(x,t)\big)$ in Eq.(3.25) and integrating both sides with $\int_{-1}^{1} dm\, m$, we have

$$\frac{\partial}{\partial t}M(x,t) = \Delta m\big[\bar{\omega}(-1,\, M(x,t),\, x,\, x+1) + \bar{\omega}(-1,\, M(x,t),\, x,\, x-1)\big] \quad (3.26)$$
$$- \Delta m\big[\bar{\omega}(+1,\, M(x,t),\, x,\, x+1) + \bar{\omega}(+1,\, M(x,t),\, x,\, x-1)\big].$$

In stationary state, we obtain the following equality

$$\Delta m\big[\bar{\omega}(-1,\, M(x),\, x,\, x+1) + \bar{\omega}(-1,\, M(x),\, x,\, x-1)\big] \quad (3.27)$$
$$- \Delta m\big[\bar{\omega}(+1,\, M(x),\, x,\, x+1) + \bar{\omega}(+1,\, M(x),\, x,\, x-1)\big] = 0.$$

We evaluate this equality for a possible configuration. In the last section, we gave the criticality condition. Let us recall Eq.(3.24)as follows:

$$\frac{a_0}{a_1} = -\big[\, 4\cos^2(\pi\ell/L) + 1\,\big]. \quad (3.28)$$

So, depending on the value of ℓ we have different a_0/a_1 value so that the critical temperature varies. Consider $M(x)$ along the lattice size L with the period λ. Let us choose the period of $M(x)$ is 10 ($\lambda = 10$) so that $\ell = L/10$. (See Figure 3.3.)

$$\cdots + \; + \; + \; + \; + \; - \; - \; - \; - \; - \cdots$$

Figure 3.3: Magnetization configuration for $\lambda = 10$: Each "+" represents positive magnetization $M(x) > 0$ and each "−" represents negative magnetization $M(x) < 0$ at certain lattice cites.

Using Eq.(3.28), the exact value of K_c is calculated for the configuration given in Figure 3.3. Table 3.3 represents K_c for each ω_x.

We calculate the value of each $M(x)$ in Figure 3.3 with the help of Eq.(3.27). We solve Eq.(3.27) self-consistently for each spin pair in one period. (We consider the spin pair and the nearest neighbors as given in Figure 2.2.)

Table 3.3: K_c values when $\ell = L/10$ for each ω_x.

ω_x	K_c
Metropolis	0.57..
Glauber	0.29..
exponential	0.22..

In the following parts, we give some important physical behaviors of the configuration shown in Figure 3.3. With the help of the self-consistent solutions, we obtain the phase boundary curves, the specific heats and the dissipated energy for each type of ω_x. We show that the critical behaviors indicate the same critical points given in Table 3.3 that we obtain exactly.

3.3.1 Phase Boundary

Let us recall Eq.(3.27) as follows:

$$\begin{aligned}&\big[\bar{\omega}(-1, M(x),\, x,\, x+1) + \bar{\omega}(-1,\, M(x),\, x,\, x-1)\big] \\ &\quad - \big[\bar{\omega}(+1,\, M(x),\, x,\, x+1) + \bar{\omega}(+1,\, M(x),\, x,\, x-1)\big] = 0.\end{aligned} \tag{3.29}$$

Here, each $\bar{\omega}$ consider eight spins and corresponding magnetization. We calculate $\bar{\omega}$'s for each $M(x)$ with $\lambda = 10$ given in the following figure.

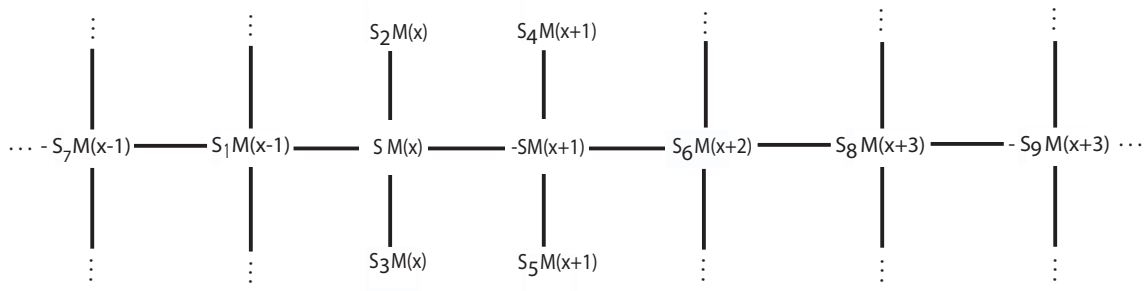

Figure 3.4: The nearest neighbor spins and the corresponding magnetization: S is one of the "+" and the "-" of the configuration we interpreted in Figure 3.3.

We calculate $M(x)$, $M(x \pm 1)$, and $M(x \pm 2)$ self-consistently with Eq.(3.29). Depending on the temperature K, we obtain that $M(x-1) = M(x+1)$ and $M(x-2) = M(x+2)$ due to the symmetry of the system (transitionally invariant lattice) and the periodic boundary condition. We evaluate the variation of $M(x)$ with respect to K. The critical behavior are consistent with the exact value given in Table 3.3. However, for the Metropolis case we obtain a discontinuity around $K \sim 0.65$ which we have not studied extensively. So, we are not sure whether this discontinuity is due to a numerical error or an indication for a second phase transition point. We note that this behavior affects our other results which depend on this magnetization curve such as specific heat and dissipated energy.

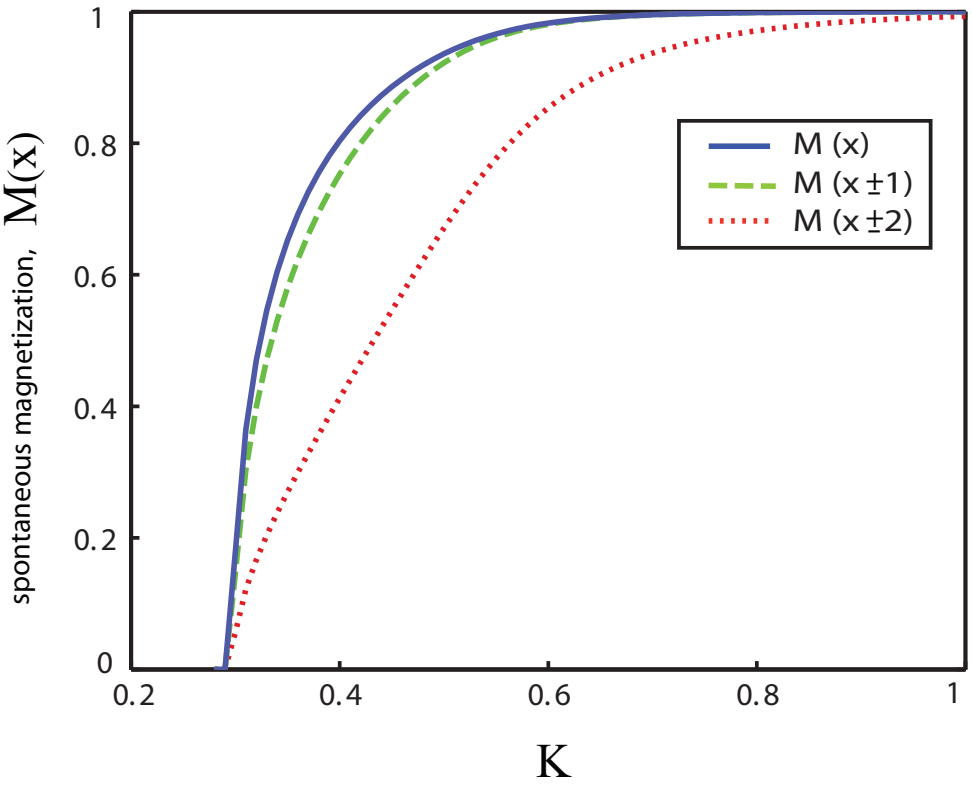

Figure 3.5: The longitudinal segregation of the Glauber rate for $\ell = L/10$: The critical behavior is obtained at $K = 0.29$ which is same as the exact value.

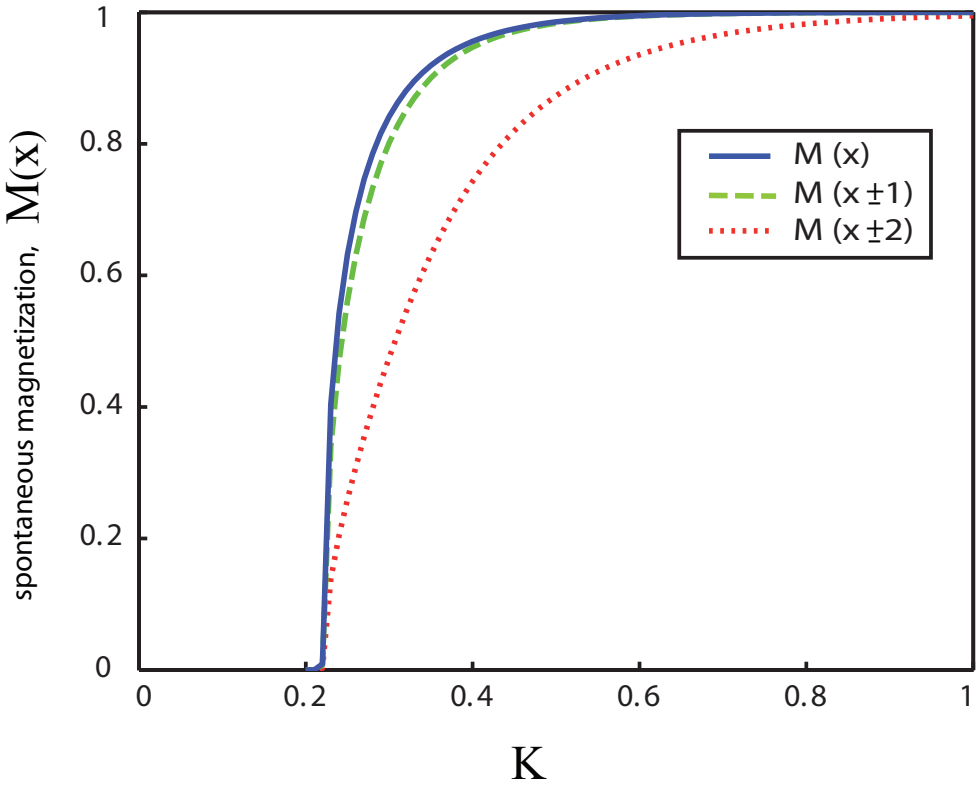

Figure 3.6: The longitudinal segregation of the exponential rate for $\ell = L/10$: The critical behavior is obtained at $K = 0.22$ which is same as the exact value.

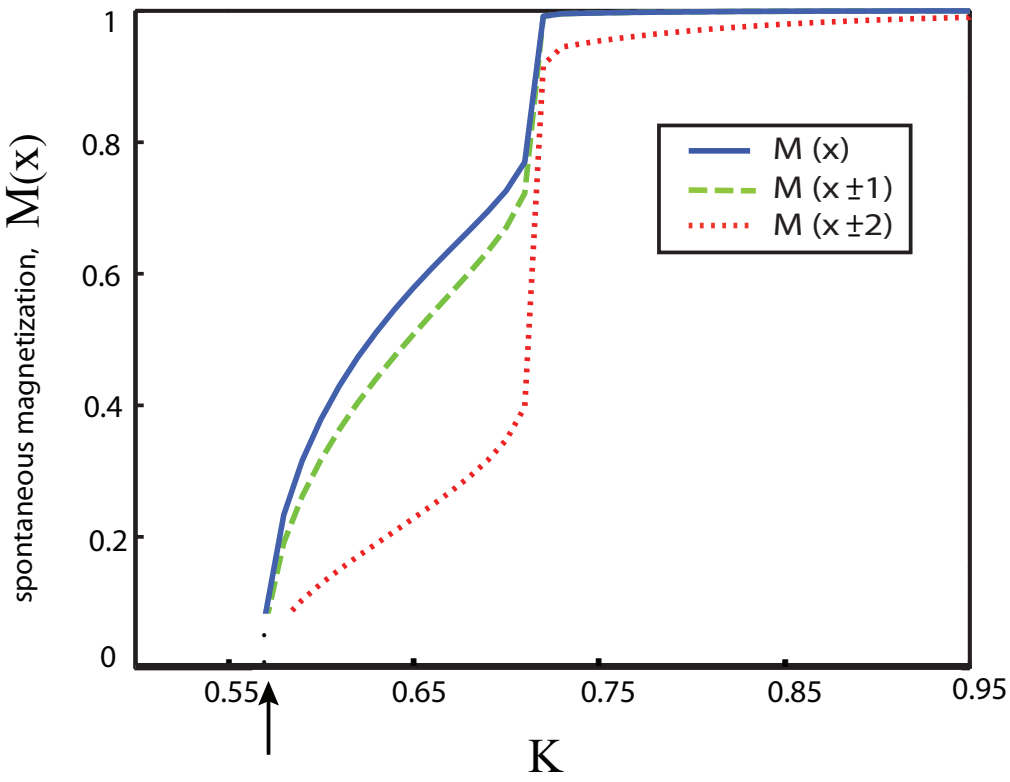

Figure 3.7: The longitudinal segregation of the Metropolis rate for $\ell = L/10$: The critical behavior is expected to be obtained at $K = 0.57$ which is shown by the arrow.

3.3.2 Specific Heat

We calculate average energy of the system with the results of spontaneous magnetization given in the last part. We consider the energy for each nearest neighbor spin pair given in Figure 3.4. So, the average energy $\langle E \rangle$ is

$$\langle E \rangle = -J \sum_{\langle ij \rangle} \langle S_i S_j \rangle. \tag{3.30}$$

We have different spin exchange kinematics in x and y directions so that the average in Eq.(3.30) should be considered the difference. Since we consider the same magnetization $M(x)$ for each column, the average of the product of any two neighboring spins with same $y-$coordinate with $x-$coordinates x and $x \pm 1$ is $\langle S_i S_j \rangle = M(x)\ M(x \pm 1)$. The average of the product of any two spins with same $x-$coordinate is $\langle S_i S_j \rangle = M(x)\ M(x)$ since the fast exchange along $y-$ direction randomizes the spins. So, we have

$$\langle E \rangle = -J\, N\big[M(x)\, M(x) + M(x)\, M(x+1)\big]. \tag{3.31}$$

Specific heat then is written as follows:

$$C_v = N\, k_B\, K^2\, \frac{\partial}{\partial K} \big[M(x)\, M(x) + M(x)\, M(x+1)\big]. \tag{3.32}$$

The following figure shows the scaled specific heat $\widetilde{C}_V = C_V / N k_B K^2$ with respect to K for each type of ω_x.

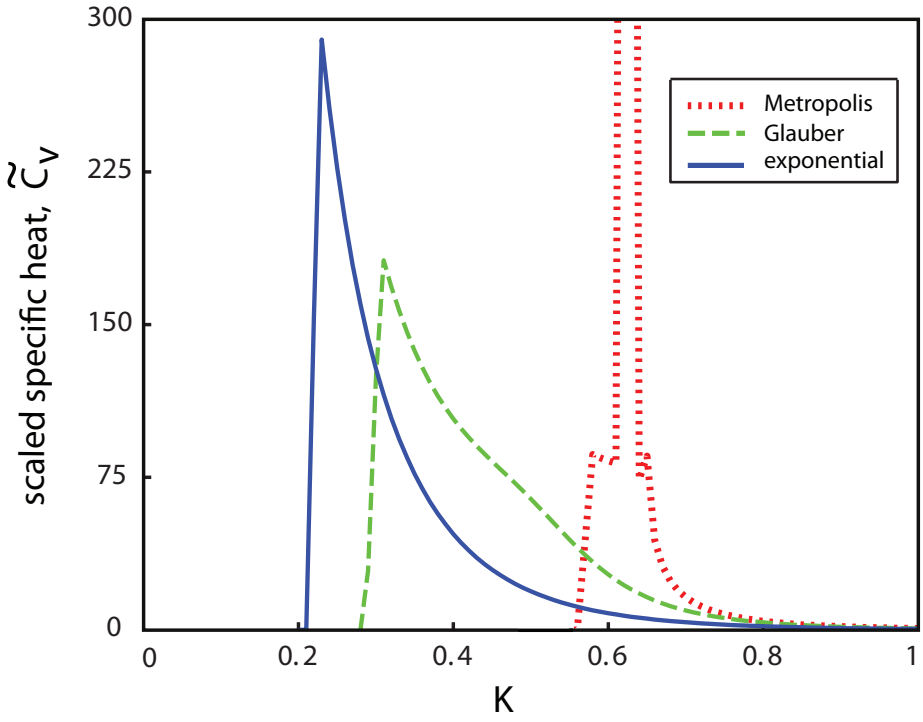

Figure 3.8: Scaled specific heats with respect to K are shown for each type of ω_x.

3.3.3 Dissipated Energy

We now consider the energy dissipation due to the spin exchanges. Heat is absorbed from the infinite temperature bath and released into the finite temperature bath. We study the energy released into the finite temperature bath by looking at the change in energy per unit time in the slow exchange process. We define the dissipated energy $(\Delta E/\Delta t)$ as follows:

$$\frac{\Delta E}{\Delta t} = 2\,N \sum_{S,\, S_1 \cdots S_6} H(S, -S)\, \bar{\omega}(S,\, m,\, x,\, x+1). \tag{3.33}$$

The following figure show the dissipated energy per a spin exchange $(\Delta E/N\Delta t)$ with respect to K for each type of ω_x.

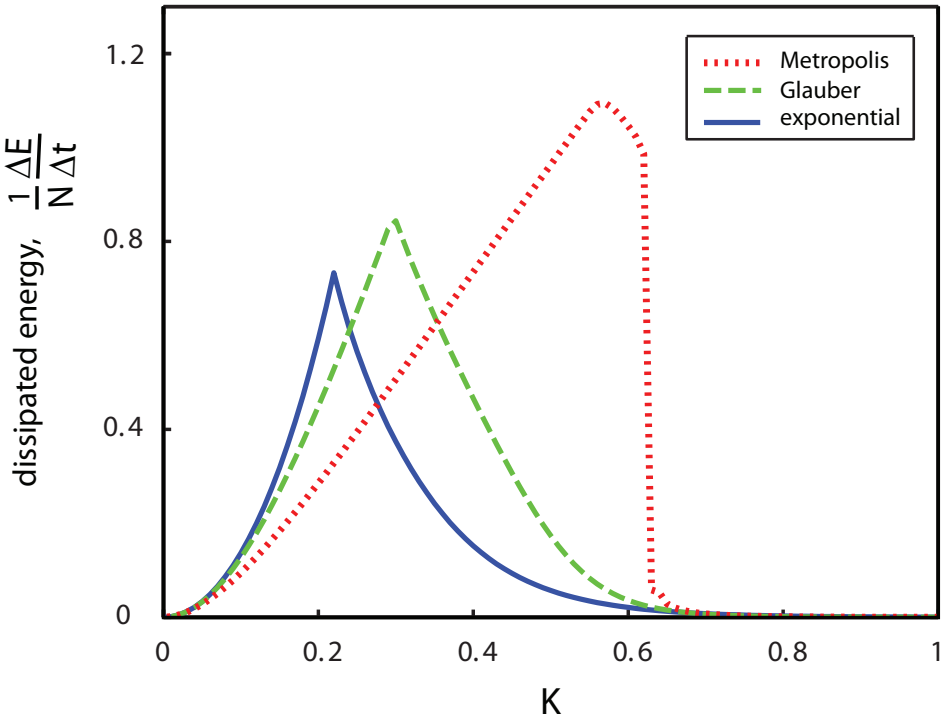

Figure 3.9: The dissipated energies per a spin exchange with respect to K are shown for each type of ω_x.

Chapter 4

CONCLUSION AND FUTURE WORK

The model we introduced gives the exact solutions near the critical points which is the significance of our study. Using various exchange dynamics, we obtain different nonequilibrium stationary states and phase behaviors. The cooperative understanding of such results is important for nonequilibrium systems since some studies [17, 18, 19] showed that the microscopic variations affect the macroscopic behavior of the systems near nonequilibrium critical points contrary to the equilibrium case. On the other hand, some nonequilibrium studies [36] asserted that the phase behaviors of such microscopically different systems fall into the same universality class. So, in order to obtain further understanding of our model in phase transitions, a Renormalization Group study is essential to analyze the universality class, which is still unknown.

Even though we did not analyze the order of transitions in detail, the phase boundary curves show that the transitions are second order. In Metropolis case, we find a discontinuity at $K \sim 0.65$ which suggests the possibility of a first order transition. However, it is not clear that whether this discontinuous phase behavior occurs due to a numerical error or an actual phase point. Further study is required to clarify this point.

We observe two kinds of phase transitions, transverse segregation and longitudinal segregation. We calculate phase transition points K_c which correspond to temperatures higher than the isotropic equilibrium temperature corresponding to $K_{\text{eq}} \sim 0.44$ for longitudinal segregation. These results are consistent with the results of the Monte Carlo simulations (see Ref. [32, 41]). We find that the longitudinal segregation occurs at a higher temperature than transverse segregation. However, we have not studied the possibility of coexistence of the two types of segregation at some K. The Monte Carlo simulations could clarify the possibility of this coexistence.

Bibliography

[1] E. L. Præstgaard, B. Schmittmann, and R. K. P Zia, Eur. Phys. J. B **18**, 675 (2000).

[2] W. B. Russel and A. P. Gast, J. Chem. Phys. **84**, 1815 (1986).

[3] L. P. Kadanoff, Rev. Mod. Phys. **71**, 435 (1999); P. G. de Gennes, Rev. Mod. Phys. **71**, S374 (1999); H. M. Jaeger, S. R. Nagel, and R. P. Behringer, Rev. Mod. Phys. **68**, 1259 (1996).

[4] G. M. Whitesides and M. Boncheva, Proc. Natl. Acad. Sci. USA **99**, 4769 (2002).

[5] E. Karsenti, Nature Rev. Mol. Cell Biol. **9**, 255 (2008).

[6] A. De Masi, P. A. Ferrari, and J. L. Lebowitz, Phys. Rev. Lett. **55**, 1947 (1985).

[7] H. Hinrichsen, Adv. Phys. **49**, 815 (2000).

[8] T. Leppänen, *Current Topics in Physics* (edited by R. A. Barrio and K. K. Kaski), Imperial College Press, UK, 2004.

[9] V. Castets, E. Dulos, J. Boissonade, and P. De Kepper, Phys. Rev. Lett. **64**, 2953 (1990).

[10] M. C. Cross and P. C. Hohenberg, Science **263**, 1569 (1994); D. A. Egolf, Science **287**, 101 (2000); M. Hildebrand, A. S. Mikhailov, and G. Ertl, Phys. Rev. E **58**, 5483 (1998).

[11] G. Odor, Rev. Mod. Phys. **76**, 663 (2004).

[12] M. Johnson, Phys. Rev. Lett. **70**, 2142 (1993); Y. Laosiritaworn, S. Ananta, and R. Yimnirun, Phys. Rev. B **75**, 054417 (2007) for the Monte Carlo study of the ferromagnetic thin film.

[13] F. Giazotto, F. Taddei, P. D'Amico, R. Fazio, and F. Beltram, Phys. Rev. B **76**, 184518 (2007).

[14] O.-P. Saira, M. Meschke, F. Giazotto, A. M. Savin, M. Möttönen, and J. P. Pekola, Phys. Rev. Lett. **99**, 027203 (2007).

[15] L. Schmidt-Mende, A. Fechtenkötter, K. Müllen, E. Moons, R. H. Friend, and J. D. MacKenzie, Science **293**, 1119 (2001).

[16] A. S. Mihailov and G. Ertl, Science **272**, 1596 (1996).

[17] P. L. Garrido and M. A. Muñoz, Phys. Rev. Lett **75**, 1875 (1995).

[18] P. L. Garrido, J. Marro, and J. M. González-Miranda, Phys. Rev. A **40**, 5802 (1989).

[19] W. Kwak, D. P. Landau, and B. Schmittmann, Phys. Rev. E **69**, 066134 (2004).

[20] R. Peierls, Proc. Camb. Phil. Soc. **32**, 477 (1936).

[21] E. Ising, Zeits. f. Physik **31**, 253 (1925).

[22] L. Onsager, Phys. Rev. **65**, 117 (1944).

[23] C. N. Yang, Phys. Rev. **85**, 808 (1952).

[24] K. G. Wilson, Phys. Rev. B **4**, 3174, 3184 (1971); see also Rev. Mod. Phys. **47**, 773 (1975) and Rev. Mod. Phys. **55**, 583 (1982) (Nobel Prize Lecture).

[25] S.-K. Ma, Phys. Rev. Lett. **37**, 461 (1976).

[26] K. Binder, Phys. Rev. Lett. **47**, 693 (1981).

[27] M. E. Fisher, Rep. Prog. Phys. **30**, 615 (1967).

[28] H. E. Stanley, Rev. Mod. Phys. **71**, S358 (1999).

[29] K. Huang, *Statistical Mechanics*, John Wiley, New York, 1987.

[30] N. Metropolis, A. W. Rosenbluth, M. N. Rosenbluth, A. H. Teller, and E. Teller, J. Chem. Phys. **21**, 1087 (1953).

[31] R. J. Glauber, J. Math. Phys. **4**, 294 (1963).

[32] H. van Beijeren and L. S. Schulman, Phys. Rev. Lett. **53**, 806 (1984).

[33] P. L. Garrido, A. Labarta, and J. Marro, J. Stat. Phys. **49**, 551 (1987).

[34] M. C. Marques, J. Phys. A **22**, 4493 (1989).

[35] T. Tomé, M. J. de Oliveria, and M. A. Santos, J. Phys. A **24**, 3677 (1991).

[36] P. Tamayo, F. J. Alexander, and R. Gupta, Phys. Rev. E **50**, 3474 (1994).

[37] R. H. Swendsen and J-S Wang, Phys. Rev. Lett. **58**, 86 (1987).

[38] P. L. Garrido, J. L. Lebowitz, C. Maes, and H. Spohn, Phys. Rev. A **42**, 1954 (1990).

[39] K.-t. Leung, B. Schmittmann, and R. K. P. Zia, Phys. Rev. Lett. **62**, 1772 (1989).

[40] M. A. Muñoz and P. L. Garrido, Phys. Rev. E **50**, 2458 (1994).

[41] K. E. Bassler and Z. Rácz, Phys. Rev. Lett. **73**, 1320 (1994); K. E. Bassler and R. K. P. Zia, J. Stat. Phys. **80**, 499 (1995).